Received <day> <Month>, <year>; | Revised <day> <Month>, <year>; | Accepted <day> <Month>, <year>

DOI: xxx/xxxx

ARTICLE TYPE

A Fast Protection Scheme for TCSC Compensated Transmission Line Using Wavelet-Alienation-Neural Technique

Bhuvnesh Rathore[1] | Amit Kumar Gangwar[2] | Om Prakash Mahela[3] | Baseem Khan[4] | Sanjeevikumar Padmanaban[5]

[1]Jodhpur Institute of Engineering Technology,Jodpur, India
[2]Government Engineering College, Jhalawar, India
[3]Power System Planning Division, Rajasthan Vidyut Prasaran Nigam Ltd., Jaipur, India
[4]Department of Electrical Engineering, Hawassa University Ethiopia
[5]CTiF Global Capsule, Department of Business Development and Technology, Aarhus University, Herning, 7400, Denmark

Correspondence
*Bassem Khan, Hawassa University Ethiopia. Email: baseem.khan04@gmail.com

Present Address
Hawassa University Ethiopia

Abstract

This paper proposes a security algorithm based on the wavelet-alienation-neural technique for detecting, classifying, and locating faults on Thyristor-Controlled Series compensator (TCSC) compensated lines. A fault index has been calculated using wavelet transform and alienation coefficients with post-fault current signals measured/sampled for quarter cycle time at both near and far end buses for fault detection and classification. The location of the fault is predicted using an Artificial Neural Network (ANN) after the fault has been diagnosed. Approximate coefficients (quarter cycle time) of both voltage and current signals, from both buses, were provided as input to ANN. Various case studies, such as variations in TCSC position, fault location, sampling frequency, power flow path, incipient angle of fault, TCSC control strategy, fault resistance, and load switching conditions, have verified the robustness of the proposed safety system.

KEYWORDS:
Neural Network, Fault diagnosis, Alienation Coefficients, TCSC, Wavelet Transform

1 | INTRODUCTION

The transmission system is in charge of transporting electricity from the generator to the power system's consumers/distribution end. For the power system to be stable and cost-effective, the transmission system must be both reliable and efficient. Flexible alternating current transmission system (FACTS) devices can improve power transfer ability and efficiency in advanced power systems (PQ). The TCSC is a series-connected compensation unit for reactive power control in transmission systems. Based on the apparent impedance measured at any given moment, the presence of TCSC within the fault loop can cause the distance relay to under-reach or over-reach. As a result, it is necessary to investigate the capabilities of signal processing and artificial intelligence techniques to resolve the limitations of traditional distance security schemes[1].

For transmission systems with series compensation, various protection scheme algorithms (PSAs) have been published in the past. Centered on the fundamental frequency and non-linear state-space dynamics, Jovcic et al. proposed various TCSC models[2]. Refs.[3] and[4] by Sidhu and Khederzadeh illustrate a detailed study of TCSC impact on the distance relaying system. Jena, et al. showed how the TCSC's impedance provided during fault transients could cause zone-2 and zone-3 operations of

[0]Bhuvnesh Rathore is with EE Department, JIET Jodpur, India (e-mail: pg201384006@iitj.ac.in); Amit Kumar Gangwar is with Government Engineering College, Jhalawar, India (e-mail: gangwar.1@iitj.ac.in); Om Prakash Mahela is with Rajasthan Vidyut Prasaran Nigam Ltd., Jaipur, India (e-mail: opmahela@gmail.com); Baseem Khan is with Hawassa University Ethiopia, (e-mail:baseem.khan04@gmail.com);Sanjeevikumar Padmanaban is with CTiF Global Capsule, Department of Business Development and Technology, Aarhus University, Herning, 7400, Denmark (e-mail: sanjeevi_12@yahoo.com)

distance relay to fail[5]. For series compensated transmission lines, Xuanwei, et al.[6] proposed a differential equation-based distance relay scheme.

Zonkoly and Desouki[7] proposed a fault diagnosis and discrimination algorithm based on wavelet entropy for FACTS paid transmission lines. Samantaray[8] proposed a new decision tree-based method for fault zone detection and fault classification in FACTS-based transmission lines. Samantaray et al. proposed an S-transform based safety algorithm for TCSC-compensated lines that uses differential energy as well as the spectral energy content of the receiving and transmitting end current signals[9]. Refs.[10] and[11] demonstrated fault classification strategies based on support vector machines. Giovanni, et al.[12] proposed a fault position algorithm that relied on sides' voltage and current signals as well as a heuristic procedure. In both the time and frequency domains, the wavelet transform proved to be useful for analyzing transients. Dash and Samantaray[1] proposed a fault analysis algorithm based on discrete wavelet transform for segment determination and step selection. Samantaray and Dash suggested wavelet-based digital depending for series compensated lines[13]. Goli et al. proposed a wavelet-based transmission line safety scheme with UPFC compensation in[14]. Masoud and Mahfouz[15] proposed a safety scheme that used alienation coefficients for existing signals from local buses. Shaik, et al.[16] proposed a wavelet transform and alienation coefficients-based defense scheme. Refs.[17,18,19] suggested a total fault diagnosis algorithm based on wavelet-alienation technique. Costa, et al.[20] published a security algorithm that accounts for the effects of fault incipient angles.

Therefore, a robust Protection Algorithm, which overcomes the demerits of speed is introduced in the manuscript and following are the main contributions::

- A fault-diagnosing algorithm for the TCSC compensated transmission line that can diagnose faults in a quarter cycle.
- The detection and classification of the faults have been achieved by wavelet based alienation technique, applied to both the bus signal data
- The 3-ϕ approximate decomposition of voltage and current signals, sampled for a quarter cycle time, are used as input to ANN to predict the fault location accurately
- Proposed algorithm is robust over different fault conditions like varying location, TCSC location, TCSC operating modes, load switching, sampling frequency, incidence angle, power-flow direction and fault resistance

The paper is organized in 7 sections. In Section-2, proposed test system and wavelet-alienation based protection algorithm are discussed. Section-3 presents algorithm demonstration for fault diagnosis and fault type identification strategies for different faults. Case studies have been demonstrated in section-4. Estimation of fault location is presented in section-5. The ability of proposed algorithm to be successful, in absence of TCSC, is demonstrated in section-6. Section-7 presents the conclusion.

2 | PROPOSED TEST SYSTEM AND ALGORITHM

Proposed test system and algorithm are described in this section.

2.1 | Test System

The pictorial view of the system, under consideration, is illustrated in Fig. 1, with parameters in Table- I[6]. The TCSC is connected at the centre of the line, rated 500kV, 60 Hz.

2.2 | Algorithm

For proposed protection scheme, 3-ϕ current signals are sampled and analyzed to obtain approximate coefficients. The alienation coefficients can be calculated using equation-1 and 2[19], discussed below:

$$A_a = 1 - r_a^2 \tag{1}$$

where, r_a refers to correlation coefficient, can be computed with the help of equation (4) as follows:

$$r_a = \frac{N_s(\sum x_a y_a) - (\sum x_a)(\sum y_a)}{\sqrt{[N_s \sum x_a^2 - (\sum x_a)^2][N_s \sum y_a^2 - (\sum y_a)^2}} \tag{2}$$

TABLE 1 SYSTEM PARAMETERS

AC Systems of both the buses	
Positive Sequence Impedance	$Z_1 = 1.43 + j16.21\Omega$
Zero Sequence Impedance	$Z_0 = 3.068 + j28.746\Omega$
Transmission Line (300 km)	
Positive Sequence Impedance Positive Sequence Parallel capacitive reactance	Z1= 0.0185 + j0.3766 Ω/km X1= 0.22789 MΩkm
Zero Sequence Impedance Zero Sequence Parallel Capacitive Reactance	$Z_0 = 0.3618 + j1.2277\Omega/km$ $X_0 = 0.34513 M\Omega km$
TCSC	
C(main)	0.000176 F
L (TCR)	0.009 H
$L_d(bypassCB)$	0.0002 H
MOV I_ref	10000 A
MOV V_ref	338000 V

where, N_s = no. of samples in a quarter cycle
x_a= array of low A-1 coefficients obtained from window-W_0.
y_a=array of A-1 coefficients obtained from window-W_{-1},
($T = 16.67ms$).

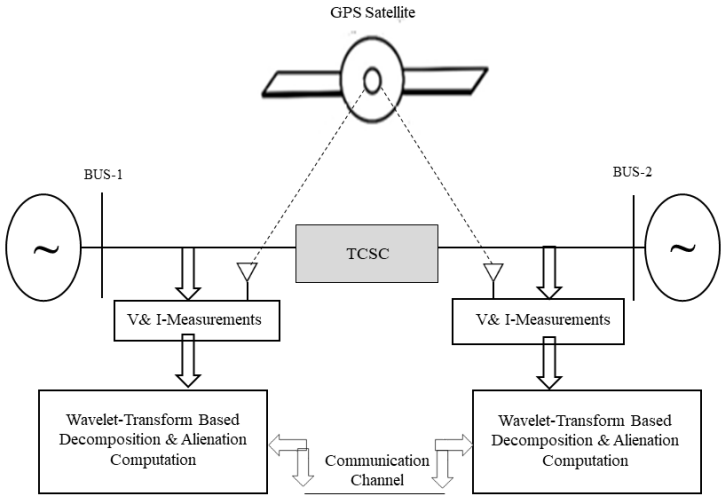

FIGURE 1 TCSC-Compensated Transmission System

The voltage and current signals of near end and far end buses are measured and sampled at 1920 Hz. The signals are embedded with time signatures also i.e. they are synchronized using Global Positioning Satellite (GPS) clock. The current signals, sampled for quarter cycle time, are analyzed with wavelet transform to extract low frequency components i.e. approximate coefficients. The alienation coefficients are calculated using these coefficients of window W_0 with those of window W_{-1}, which are separated

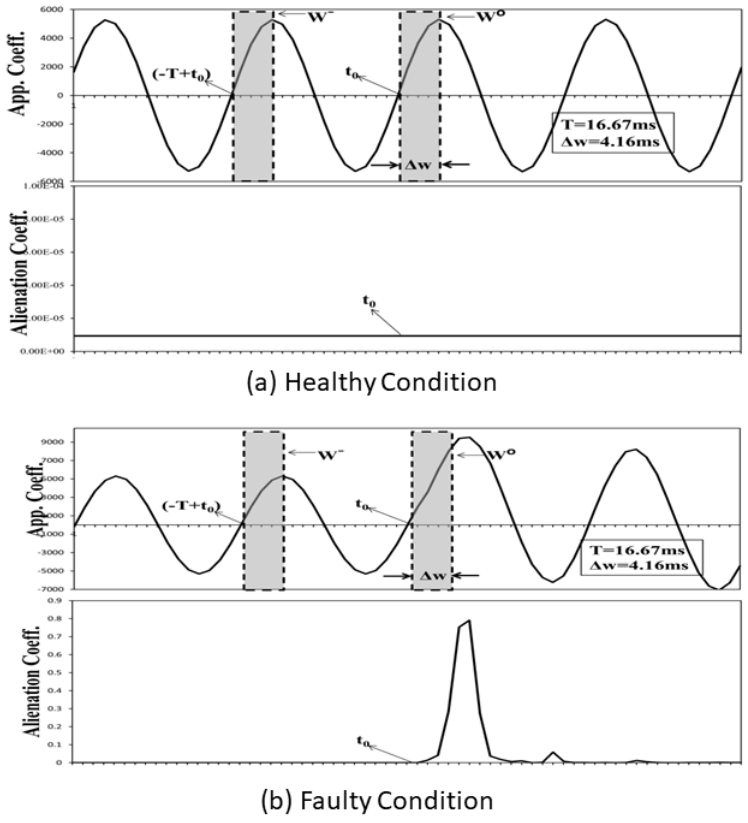

FIGURE 2 Illustration of Alienation Coefficients Computation (a) healthy condition (b) faulty condition

by a cycle, which is clear from Fig. 2. Fault Index (FI) is determined by summing up alienation coefficients obtained from both the buses.

Under healthy conditions, the alienation coefficients obtained from windows W_0 and W_{-1}, will have zero value (and hence the FI) due to similarity of signals captured as illustrated in Fig. 2(a). But, for faulty condition, it will reach upto a non-zero value (and hence the FI), due to the variations in the approximate coefficients windows compared. This FI, is used as a tool, by comparing it with a threshold (F-TH = 0.1) value to diagnose the fault. The steps of the proposed algorithm can be explained by flow chart of Fig. 3.

3 | ALGORITHM DEMONSTRATION

The safety algorithm steps for phase-A to Ground fault are shown in Figure 4. Figure 4 (a) and (b) display the existing signals of both buses. Following the existing signals, the approximate coefficients of respective buses are shown in Figures 4(c) and 4(d). Figures 4(e) and 4(f) display plots of alienation coefficients calculated from Fig. 4(c) and 4(d) coefficients, respectively. Figure 4 (g) shows the FI variance obtained by adding the alienation coefficients from Figures 4(e) and (f). With this FI, it's important to note that only phase-value A's exceeds the threshold and not for phases B and C. As a result, it's diagnosed as a phase-A to Ground fault or AG fault.

Faults may also be identified solely by FI after they have been detected. FI variation of three-phases for AB, ABG, and ABCG faults is depicted in Fig. 5. Figures 5(a) and 5(b) show that the FI value for the defective phases (A and B) is greater than the threshold, indicating that the fault is two-phase. The fact that all phases have FI values greater than the threshold is significant in Fig. 5(c). As a result, it is classified as a three-phase fault.

However, the proposed FI will not be able to distinguish between line to line (AB) and line to line to ground (ABG) faults. This is because for any two-phase fault, whether with or without ground, the FIs of those two phases will be greater than the

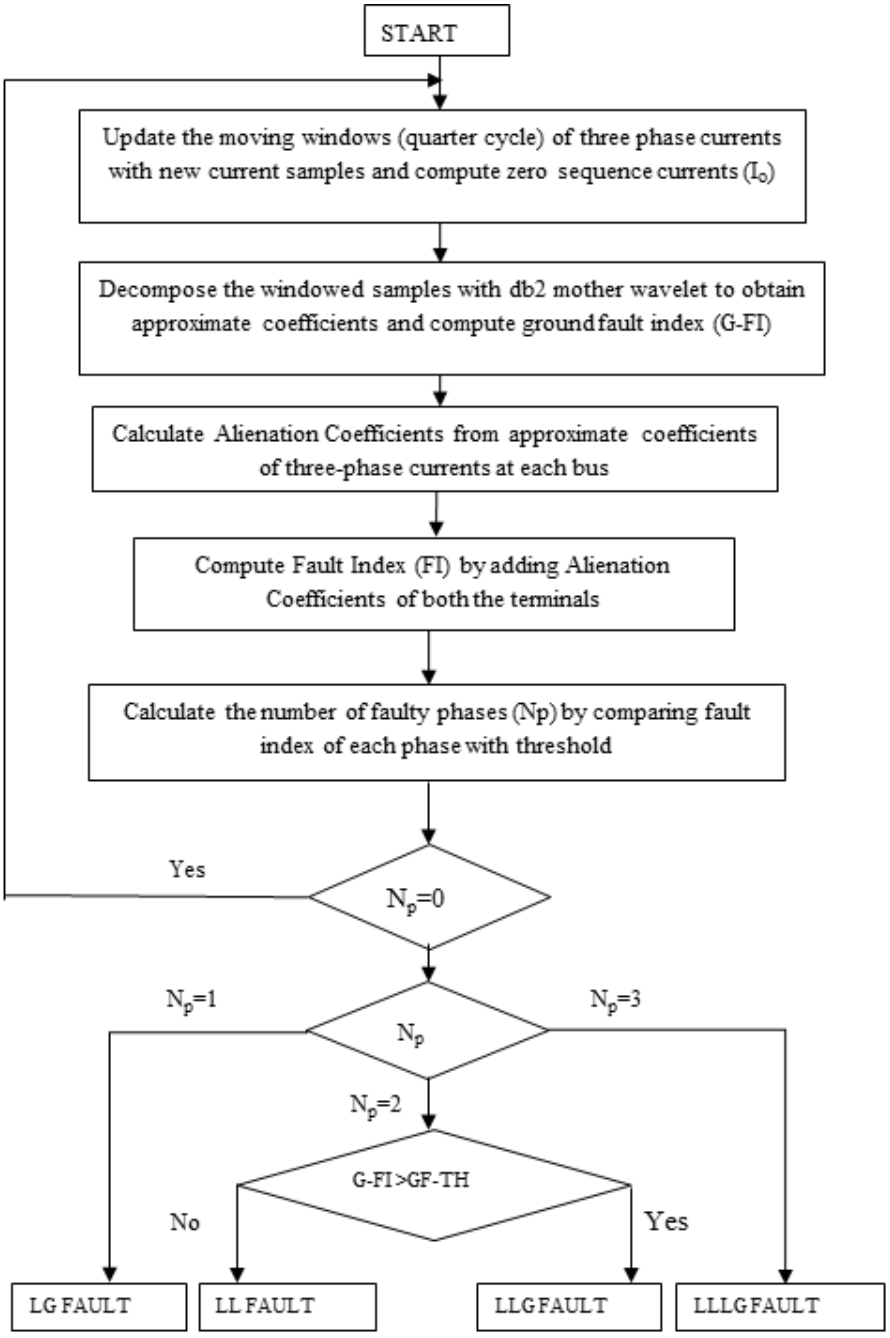

FIGURE 3 Steps for Proposed Algorithm

threshold, making it impossible to differentiate faults with or without ground. With the aid of neutral current, a ground fault index (G-FI) is proposed for distinguishing two phase faults with and without ground. The G-FI plot vs. time for AB and ABG faults is shown in Fig.5 (d), and it can be shown that the G-FI value for AB fault is much lower than the threshold to be found, while the value for ABG fault is much higher and important.

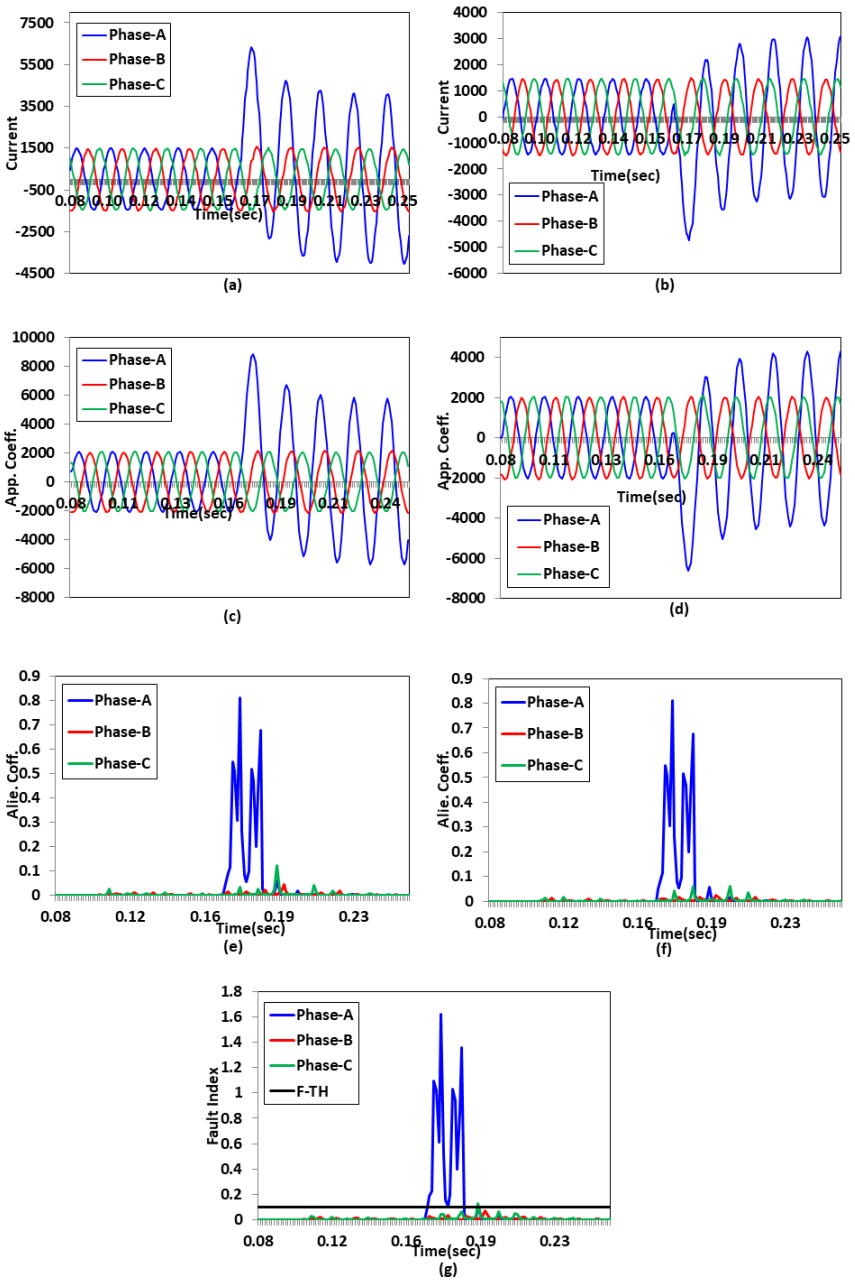

FIGURE 4 AG-Fault Diagnosis Demonstration: (a) & (b) 3-ϕ current signals of bus-1 and 2 respectively, (c) & (d) approximate coefficients of respective buses, (e) & (f) respective buses' alienation coefficients and (g) FI variation

4 | CASE STUDIES

The performance of reported protection algorithm has been tested for different faults by case studies of varying location, TCSC location, TCSC operating modes, load switching, sampling frequency, incidence angle, power-flow direction and fault resistance.

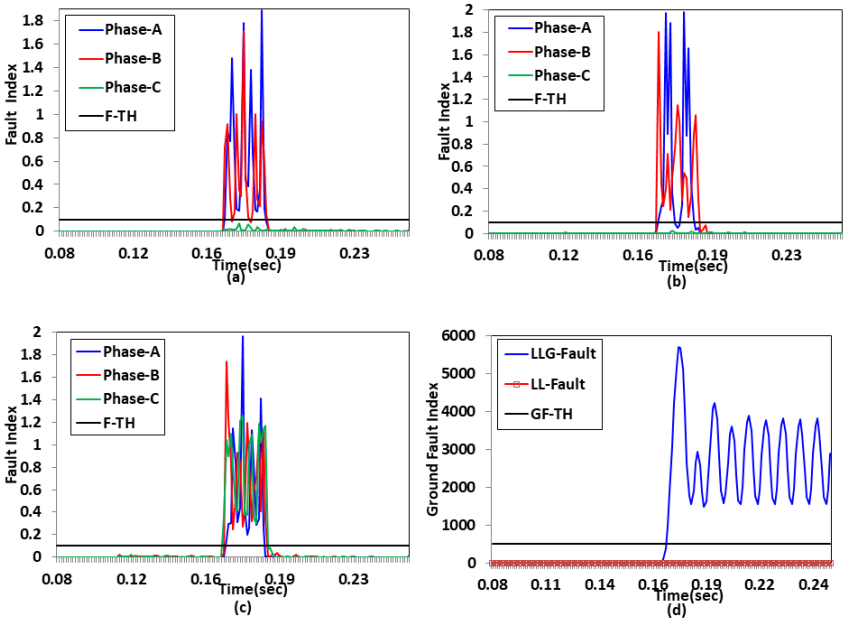

FIGURE 5 FI Variation for different faults and G-FI (a) AB fault (b) ABG fault (c) ABCG fault (d) G-FI for discriminating AB and ABG faults

4.1 | Fault Location Variation

The fault transients/ signals varies largely/significantly with fault locations, thus it is must to test the reported scheme for varying locations of fault. The faults have been created for every 20 kms along the length of the line. From Fig. 6(a), it is observed that FI value for phase-A (which is faulty phase) is larger as compared to the F-TH while not for B C (which are healthy phases), it signifies the fault identified as AG fault. From Fig 6(b) & 6(c), it is noticed that the variation of FI values for phases-A and B are always higher w.r.t. the F-TH, for AB and ABG faults, everywhere while the FI value of C-phase is very much lower as compared to the threshold. From Fig. 6(d), it can be significantly noticed that the FIs values of all the 3-ϕ remain higher w.r.t. the threshold for 3-ϕ fault at various locations. Thus, the proposed algorithm works for variations in fault location also.

4.2 | Fault Incidence Angle (FIA) Variation

The fault incidence angles also responsible for affecting post-fault transients that is why it has become important to test the applicability of reported scheme for varying FIA. For this purpose, FIA is varied from 0° to 180° in steps of 30°. For AG fault, detection and classification with varying FIA, FI variation is shown in Fig. 7 (a). Similarly results of FI variation, for AB and ABG faults, are illustrated in Fig. 7 (b) & (c) respectively. Fig. 7 (d) presents the FI variation plot for ABCG fault. From all the results, it is significant to observe that at different values of FIA, the FI only for faulty phase/s attain higher w.r.t. the threshold while not those of non-faulty phase/s. With these results, it can be concluded that FIA variation could not affect performance of proposed method.

4.3 | Variation of Fault Resistance (FR)

Faults with high resistances in fault path, are difficult to diagnose because of less sensitivity of relays towards less value of post fault currents. The ability of the reported protection scheme, for high impedance faults, is established by selecting FRs from 0-100Ω under this case study. Fig.8 illustrates results for different types of faults, with FR of 15Ω. Fig 8(a) depicts that the FI value of A is more as compared to the threshold and for other phases it has very much lesser value everywhere, hence it is identified as AG fault. This can be significantly distinguished from Fig. 8 (b) and (c) that for non-faulty phases i.e. A & B, FIs are more w.r.t. threshold while it is not so for the healthy phase i.e. phase-C, and they are diagnosed as AB and ABG faults. It is evident

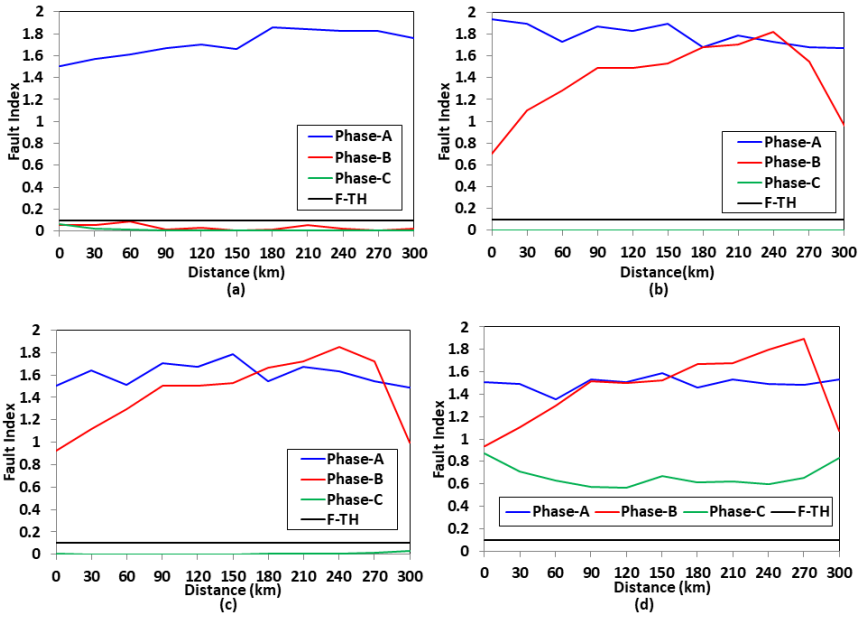

FIGURE 6 Results for various faults for fault location variations (a) AG fault (b) AB fault (c) ABG fault (d) ABCG fault

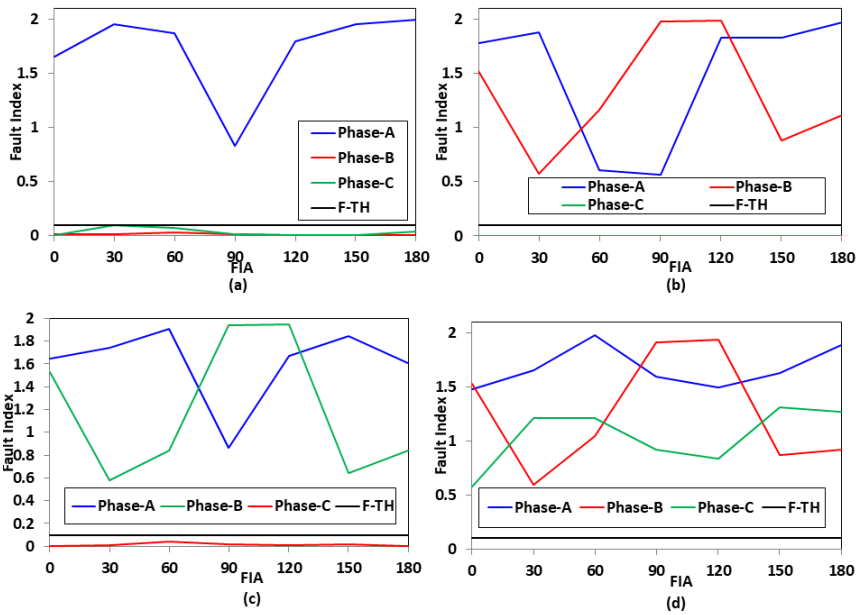

FIGURE 7 Results for various faults for different FIAs (a) AG fault (b) AB fault (c) ABG fault (d) ABCG fault

from Fig 8(d) that the FI value of all the phases is more w.r.t. threshold; hence it is identified as 3-ϕ fault. With these results, it can be made that FR variation could not influence execution of the algorithm. ‘

4.4 | Variation in TCSC Operation Modes

For proving the robustness of algorithm, it has also been tested with various operating modes of TCSC i.e. for capacitive and inductive modes, although the latter is rarely used in practice. All the results have been computed with TCSC operating in

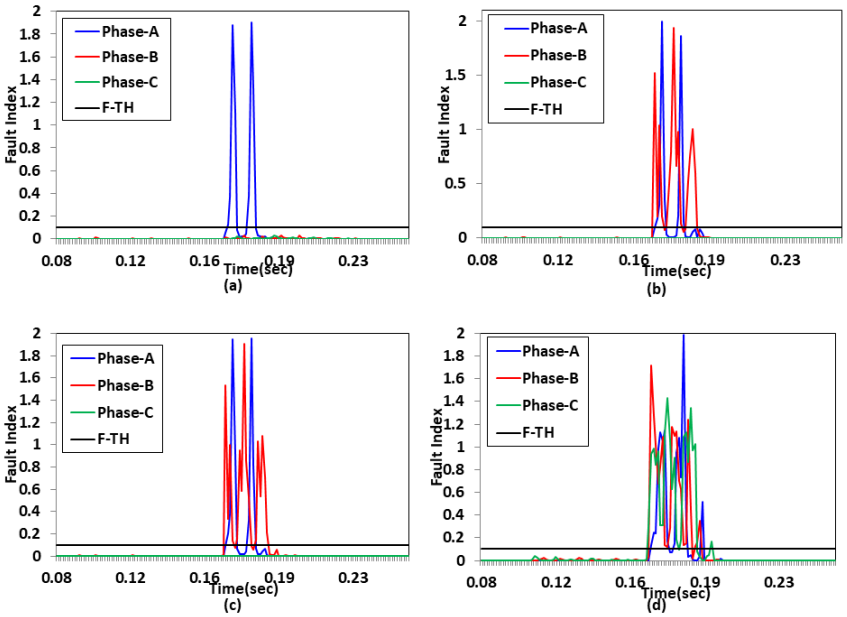

FIGURE 8 FI Variation for high impedance faults (a) AG fault (b) AB fault (c) ABG fault (d) ABCG fault

capacitive mode. Thus, in here the results are derived for inductive mode operation for TCSC. Fig.9 illustrates the fault index variation of all the 3-ϕ for different faults with TCSC operating in inductive mode. For AG fault, detection and classification with varying FIA, FI variation is shown in Fig. 9 (a). Similarly results of FI variation, for AB and ABG faults, are illustrated in Fig. 9 (b) & (c) respectively. Fig. 9 (d) presents the FI variation plot for ABCG fault. From all the results, it is significant to observe that at different values of FIA, the FI only for faulty phase/s attain higher w.r.t. the threshold while not those of healthy phase/s. Thus, it is can be significantly observed that proposed protection method's performance cannot be affected by control modes of TCSC.

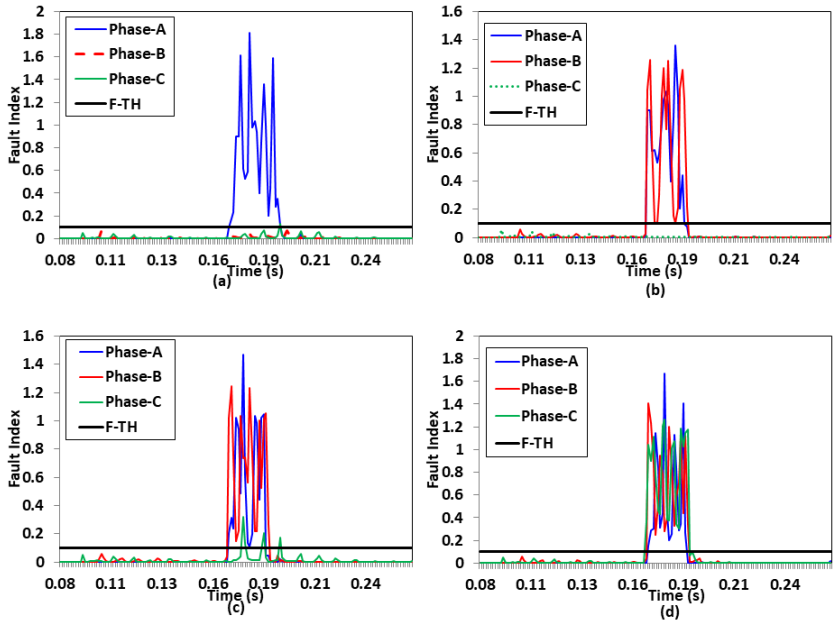

FIGURE 9 FI Variation for Inductive Mode of TCSC (a) AG fault (b) AB fault (c) ABG fault (d) ABCG fault

4.5 | Variation of TCSC location

The location of TCSC greatly affects the value of fault transients. Thus, it becomes necessary to check the algorithm applicability for different locations of TCSC i.e. middle and at receiving end. Figs. 10(a-d) presents the results of FI variation for different faults. From Fig. 10, it can be noticed that the fault index of faulty phases alone, have larger value w.r.t. the threshold and that of non-faulty phases. With these results, a conclusion can be made of robustness of algorithm for TCSC location variation.

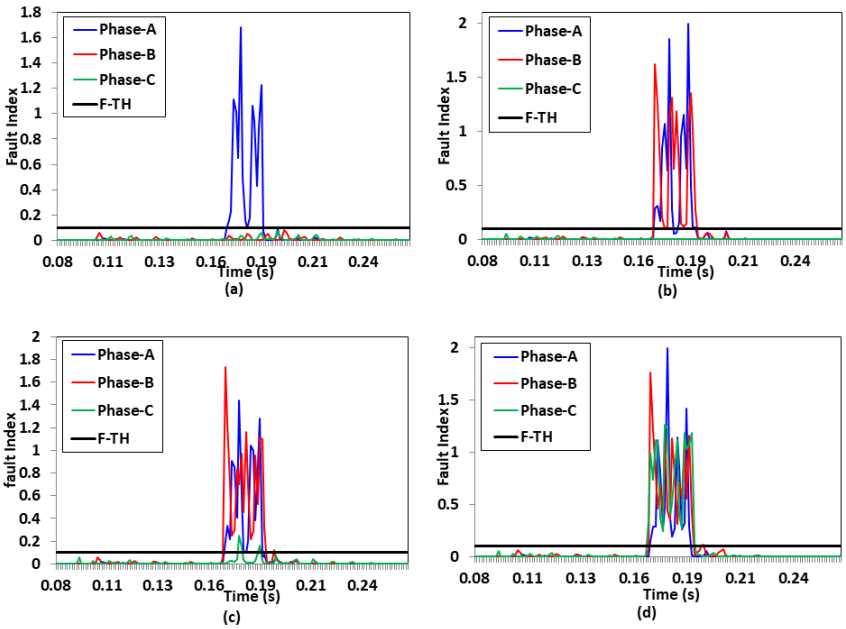

FIGURE 10 FI Variation for TCSC installed at receiving end (a) AG fault (b) AB fault (c) ABG fault (d) ABCG fault

4.6 | Effect of Noise Contamination

To demonstrate the robustness of the proposed scheme for diagnosing and classifying faults, noise is combined with current signals and used for the algorithm in a noisy environment. The ranges of SNRs considered for this reason are 40dB-10dB. Figure 11 (a) shows the FI variation for AG fault identification and classification with varying FIA. Similarly, for AB and ABG faults, the effects of FI variance are shown in Fig. 11 (b) & (c). The FI variation plot for the ABCG fault is shown in Figure 11 (d). As a result, it is clear that the proposed safety system would not fail in the face of noise pollution.

4.7 | Effect of Loading

Switching of loads also generates transients in the current signals which may affect the proposed protection algorithm, which works making use of current signals information. Hence, the execution of the reported algorithm has been checked/tested for 10% and 20% of load changes. The highest fault indexes associated with the load switching is found to be 0.07 which is very low as compared to threshold (0.10) value. Thus, it is evident that the load switching transients have no effect on proposed algorithm.

4.8 | Power-Flow Reversal

For accounting the effect of power flow reversal on given method, the position of power/ supply has been changed from bus-1 to bus-2, thus reverses the direction of current and hence power flow. Because the reported scheme makes use of data from both near end and the far end buses, that is why the new results corresponding to change in direction of power-flow, are found to be similar/significant as in case of original power flow.

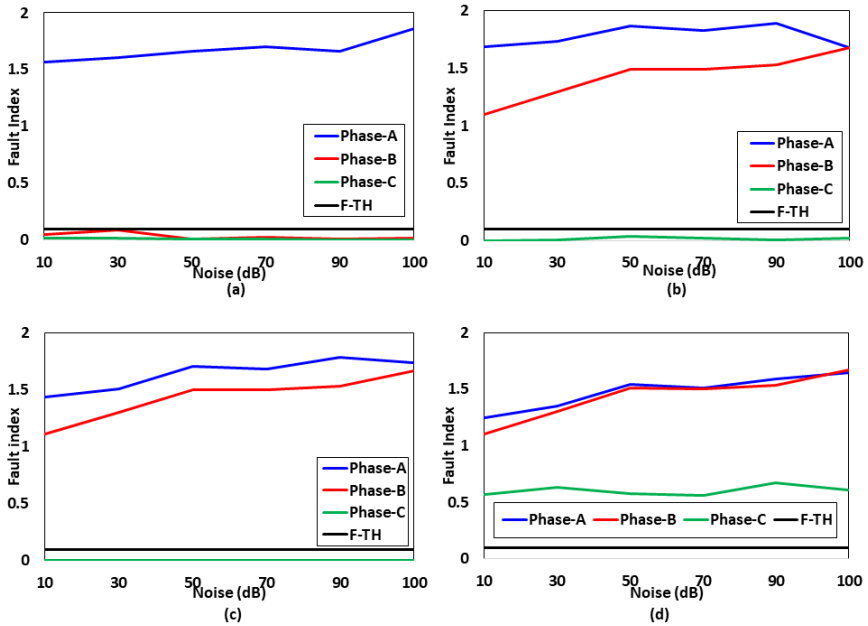

FIGURE 11 Fault Index Variation for Noisy Environment (a) AG fault (b) AB fault (c) ABG fault (d) ABCG fault

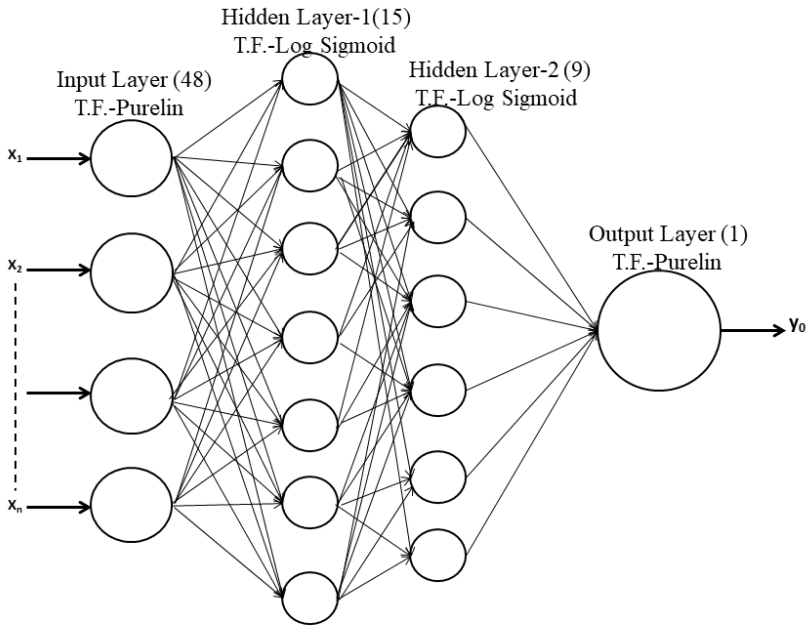

FIGURE 12 ANN Structure

4.9 | Variation of Sampling Frequency

To test the applicability of proposed scheme for varying sampling frequency, the results for fault analysis have been re-simulated with 0.96 kHz, 1.92 kHz, 3.84 kHz and 7.68 kHz as sampling frequency. It has been significantly seen that higher sampling frequencies have no considerable change in the performance w.r.t. accuracy and speed, while its reduction adversely affects the algorithm results by increasing the detection time.

5 | PREDICTION OF FAULT LOCATION

After successful diagnosis and identification of fault type, further it is required to predict the fault location precisely. For this purpose, Artificial Neural Network (ANN) has been significantly used, whose architecture is shown in Fig. 12. The input to neural network is 4-approximate coefficients, of each phase V & I signals, of a quarter cycle time, from both the ends of the line. Thus, the total number of inputs is 48 coefficients which can be computed as, 4 coefficients for each signal, for both 3-*phi* voltage and current signals (6) and for both the buses (2) i.e. $4 * 6 * 2 = 48$.

The output of the ANN will be the predicted location w.r.t. bus-1. The training of proposed ANN has been carried out by feeding data generated by simulating faults for different locations. The trained ANN has been tested for its performance with the data obtained by simulating faults with new cases. The percentage error (E) in fault location is calculated as:-

$$\%E = \frac{|L_{NN} - L_{actual}|}{L_{TL}} \tag{3}$$

Where L_{NN}: fault location predicted by Neural Network, L_{actual}: Actual Fault location and L_{TL}: Transmission line Length

Table-II demonstrates the accuracy using proposed ANN. From which, it can be observed that the maximum and average error, in locating the faults, is 1.97% and 0.81% respectively.

6 | PERFORMANCE COMPARISON

In practical field, the TCSC can be sometimes disconnected due to maintenance or outage, even in this condition/scenario also the protection system must significantly work. To test the algorithm for this type of situation i.e. in absence of TCSC, it has been simulated by disconnecting the TCSC form the system and various types of faults have been simulated and tested with given algorithm. Table-III presents the results of reported algorithm, in presence and absence of TCSC. From which, it can be clearly seen that the fault indexes of faulty phases have higher value as compared to the threshold, both in presence and absence of TCSC. Thus, it is evident that the given algorithm will not be influenced by TCSC presence or absence. Tables IV to XIII details the results of successful operation of reported algorithm for various faults at different incidence angles and with variations in fault locations.

7 | CONCLUSION

A Wavelet-Alienation-Neural based fault analysis method has been proposed for complete protection of transmission line, operating with TCSC. Approximate decomposition of current signals, obtained for quarter cycle time, are compared in terms of alienation coefficients to detect and classify faults. Prediction of fault location has been carried out by ANN, whose input is wavelet coefficients of 3-ϕ V & I signals. Thus, the proposed algorithm was found to be significant in diagnosis and classification of faults with varying location, TCSC location, TCSC operating modes, load switching, sampling frequency, incidence angle, power-flow direction and fault resistance. The faults have also been located with a fair accuracy.

8 | CONFLICTS OF INTEREST

Authors have no conflict of interest relevant to this article.

References

1. Dash P, Samantray S. Phase selection and fault section identification in thyristor controlled series compensated line using discrete wavelet transform. *International Journal of Electrical Power & Energy Systems* 2004; 26(9): 725–732.

2. Jovcic D, Pillai G. Analytical modeling of TCSC dynamics. *IEEE Transactions on Power Delivery* 2005; 20(2): 1097–1104.

3. Sidhu T, Khederzadeh M. TCSC impact on communication-aided distance-protection schemes and its mitigation. *IEE Proceedings-Generation, Transmission and Distribution* 2005; 152(5): 714–728.

4. Khederzadeh M, Sidhu TS. Impact of TCSC on the protection of transmission lines. *IEEE Transactions on power delivery* 2005; 21(1): 80–87.

5. Jena MK, Panigrahi B, Das S, Samantaray SR. Exposing zone-2 and zone-3 mal-operations in thyristor-controlled series capacitor compensated transmission system. In: IEEE. ; 2016: 1–6.

6. Qi X, Wen M, Yin X, Zhang Z, Tang J, Cai F. A novel fast distance relay for series compensated transmission lines. *International Journal of Electrical Power & Energy Systems* 2015; 64: 1–8.

7. El-Zonkoly AM, Desouki H. Wavelet entropy based algorithm for fault detection and classification in FACTS compensated transmission line. *International Journal of Electrical Power & Energy Systems* 2011; 33(8): 1368–1374.

8. Samantaray S. Decision tree-based fault zone identification and fault classification in flexible AC transmissions-based transmission line. *IET generation, transmission & distribution* 2009; 3(5): 425–436.

9. Samantaray S, Tripathy L, Dash P. Differential energy based relaying for thyristor controlled series compensated line. *International Journal of Electrical Power & Energy Systems* 2012; 43(1): 621–629.

10. Dash P, Samantaray S, Panda G. Fault classification and section identification of an advanced series-compensated transmission line using support vector machine. *IEEE transactions on power delivery* 2006; 22(1): 67–73.

11. Parikh UB, Das B, Maheshwari R. Fault classification technique for series compensated transmission line using support vector machine. *International Journal of Electrical Power & Energy Systems* 2010; 32(6): 629–636.

12. Junior GM, Di Santo SG, Rojas DG. Fault location in series-compensated transmission lines based on heuristic method. *Electric Power Systems Research* 2016; 140: 950–957.

13. Samantaray S, Dash P. Wavelet packet-based digital relaying for advanced series compensated line. *IET Generation, Transmission & Distribution* 2007; 1(5): 784–792.

14. Goli RK, Shaik AG, Ram ST. A transient current based double line transmission system protection using fuzzy-wavelet approach in the presence of UPFC. *International Journal of Electrical Power & Energy Systems* 2015; 70: 91–98.

15. Masoud M, Mahfouz M. Protection scheme for transmission lines based on alienation coefficients for current signals. *IET generation, transmission & distribution* 2010; 4(11): 1236–1244.

16. Rathore B, Shaik AG. Fault detection and classification on transmission line using wavelet based alienation algorithm. In: IEEE. ; 2015: 1–6.

17. Rathore B, Shaik AG. Fault Analysis Using Alienation Technique for Three-Terminal Transmission Line. In: IEEE. ; 2018: 1–6.

18. Rathore B. Alienation based fault detection and classification in transmission lines. In: IEEE. ; 2015: 1–6.

19. Rathore B, Shaik AG. Wavelet-alienation based transmission line protection scheme. *IET Generation, Transmission & Distribution* 2017; 11(4): 995–1003.

20. Costa F, Souza B, Brito N. Effects of the fault inception angle in fault-induced transients. *IET generation, transmission & distribution* 2012; 6(5): 463–471.

TABLE 2 Estimation of Fault Location

S.No.	Fault Type	Actual Location	ANN Location	% Error
1	Phase-A to G	21	25.35	1.45
2	Phase-A to G	93	95.86	0.95
3	Phase-A to G	169	169.50	0.17
4	Phase-A to G	217	216.46	0.18
5	Phase-A to G	275	276.24	0.41
6	Phase-B to G	21	26.92	1.97
7	Phase-B to G	93	90.09	0.97
8	Phase-B to G	169	166.17	0.94
9	Phase-B to G	217	217.06	0.02
10	Phase-B to G	275	280.61	1.87
11	Phase-C to G	21	21.16	0.05
12	Phase-C to G	93	90.70	0.77
13	Phase-C to G	169	168.08	0.31
14	Phase-C to G	217	214.25	0.92
15	Phase-C to G	275	278.73	1.24
16	Phase-A to B	21	25.09	1.36
17	Phase-A to B	93	97.42	1.47
18	Phase-A to B	169	169.91	0.30
19	Phase-A to B	217	219.25	0.75
20	Phase-A to B	275	279.05	1.35
21	Phase-B to C	21	21.05	0.02
22	Phase-B to C	93	91.21	0.60
23	Phase-B to C	169	168.63	0.12
24	Phase-B to C	217	211.73	1.76
25	Phase-B to C	275	270.87	1.38
26	Phase-A to C	21	19.89	0.37
27	Phase-A to C	93	94.25	0.42
28	Phase-A to C	169	169.35	0.12
29	Phase-A to C	217	216.76	0.08
30	Phase-A to C	275	274.28	0.24
31	Phases-AB to G	21	23.03	0.68
32	Phases-AB to G	93	92.52	0.16
33	Phases-AB to G	169	165.09	1.30
34	Phases-AB to G	217	215.97	0.34
35	Phases-AB to G	275	269.90	1.70
36	Phases-BC to G	21	23.39	0.80
37	Phases-BC to G	93	98.52	1.84
38	Phases-BC to G	169	171.27	0.76
39	Phases-BC to G	217	213.89	1.04
40	Phases-BC to G	275	280.09	1.70
41	Phases-AC to G	21	20.07	0.31
42	Phases-AC to G	93	98.13	1.71
43	Phases-AC to G	169	166.12	0.96
44	Phases-AC to G	217	217.84	0.28
45	Phases-AC to G	275	271.69	1.10
46	Phases-ABC to G	21	19.51	0.50
47	Phases-ABC to G	93	94.29	0.43
48	Phases-ABC to G	169	170.68	0.56
49	Phases-ABC to G	217	212.83	1.39
50	Phases-ABC to G	275	275.98	0.33

TABLE 3 Performance Comparison

S.No.	Fault type	A		B		C	
		Without TCSC	With TCSC	Without TCSC	With TCSC	Without TCSC	With TCSC
1	Phase-A to G	1.65	1.65	0.01	0.01	0.00	0.00
2	Phase-B to G	0.06	0.05	1.51	1.52	0.0	0.00
3	Phase-C to G	0.01	0.01	0.01	0.00	0.87	0.86
4	Phase-A to B	1.78	1.78	1.52	1.52	0.00	0.00
5	Phase-B to C	0.00	0.00	1.37	1.38	0.90	0.99
6	Phase-A to C	1.35	1.35	0.01	0.00	1.00	1.00
7	Phases-AB to G	1.64	1.64	1.52	1.53	0.01	0.00
8	Phases-BC to G	0.02	0.01	1.51	1.52	0.76	0.76
9	Phases-AC to G	1.39	1.39	0.00	0.01	1.00	0.99
10	3-ϕ fault	1.47	1.47	1.52	1.53	0.58	0.58

TABLE 4 Results of AG Fault for FI Variation with different locations and FIAs

Angle	0			30			60			90			120			150		
Distance	a	b	c	a	b	c	a	b	c	a	b	c	a	b	c	a	b	c
30	**1.57**	**0.05**	**0.02**	**1.59**	**0.28**	**0.42**	**1.61**	**0.30**	**0.12**	**1.62**	**0.15**	**0.01**	**1.63**	**0.11**	**0.01**	**1.63**	**0.14**	**0.15**
60	**1.61**	**0.09**	**0.02**	**1.63**	**0.06**	**0.23**	**1.68**	**0.04**	**0.14**	**1.65**	**0.06**	**0.03**	**1.69**	**0.03**	**0.00**	**1.70**	**0.03**	**0.01**
90	**1.66**	**0.01**	**0.01**	**1.63**	**0.06**	**0.14**	**1.73**	**0.04**	**0.16**	**1.68**	**0.02**	**0.06**	**1.73**	**0.00**	**0.00**	**1.75**	**0.02**	**0.00**
120	**1.70**	**0.03**	**0.01**	**1.67**	**0.03**	**0.07**	**1.77**	**0.06**	**0.07**	**1.75**	**0.02**	**0.04**	**1.78**	**0.00**	**0.00**	**1.78**	**0.02**	**0.00**
150	**1.66**	**0.01**	**0.00**	**1.72**	**0.03**	**0.11**	**1.79**	**0.05**	**0.07**	**1.76**	**0.01**	**0.03**	**1.79**	**0.01**	**0.01**	**1.78**	**0.01**	**0.00**
180	**1.86**	**0.02**	**0.00**	**1.67**	**0.01**	**0.05**	**1.87**	**0.02**	**0.07**	**1.87**	**0.08**	**0.05**	**1.85**	**0.01**	**0.01**	**1.82**	**0.01**	**0.00**
210	**1.84**	**0.05**	**0.00**	**1.77**	**0.01**	**0.08**	**1.83**	**0.03**	**0.13**	**1.75**	**0.03**	**0.10**	**1.88**	**0.02**	**0.03**	**1.84**	**0.01**	**0.00**
240	**1.82**	**0.02**	**0.00**	**1.73**	**0.01**	**.11**	**1.71**	**0.03**	**0.12**	**1.89**	**0.33**	**0.08**	**1.82**	**0.10**	**0.03**	**1.85**	**0.01**	**0.02**
270	**1.82**	**0.01**	**0.00**	**1.83**	**0.02**	**0.13**	**1.73**	**0.08**	**0.11**	**1.73**	**0.08**	**0.06**	**1.87**	**0.27**	**0.08**	**1.79**	**0.01**	**0.07**

TABLE 5 Results of BG Fault for FI Variation with different locations and FIAs

Angle	0			30			60			90			120			150		
Distance	a	b	c	a	b	c	a	b	c	a	b	c	a	b	c	a	b	c
30	**0.02**	**1.06**	**0.01**	**0.02**	**1.15**	**0.01**	**0.00**	**1.98**	**0.07**	**0.02**	**1.99**	**0.03**	**0.01**	**1.92**	**0.02**	**0.01**	**1.96**	**0.05**
60	**0.08**	**1.16**	**0.03**	**0.01**	**1.17**	**0.06**	**0.00**	**1.97**	**0.02**	**0.01**	**1.98**	**0.03**	**0.06**	**1.96**	**0.01**	**0.04**	**1.98**	**0.02**
90	**0.04**	**1.32**	**0.05**	**0.01**	**1.19**	**0.03**	**0.00**	**1.96**	**0.01**	**0.00**	**1.97**	**0.03**	**0.03**	**1.96**	**0.01**	**0.02**	**2.00**	**0.02**
120	**0.01**	**1.50**	**0.05**	**0.00**	**1.29**	**0.02**	**0.00**	**1.94**	**0.00**	**0.00**	**1.95**	**0.01**	**0.01**	**1.95**	**0.02**	**0.09**	**1.99**	**0.02**
150	**0.06**	**1.52**	**0.05**	**0.04**	**1.29**	**0.03**	**0.00**	**1.94**	**0.01**	**0.00**	**1.93**	**0.00**	**0.01**	**1.95**	**0.07**	**0.05**	**1.99**	**0.01**
180	**0.04**	**1.59**	**0.01**	**0.06**	**1.39**	**0.03**	**0.00**	**1.90**	**0.01**	**0.00**	**1.93**	**0.00**	**0.02**	**1.93**	**0.01**	**0.07**	**2.00**	**0.02**
210	**0.03**	**1.65**	**0.07**	**0.01**	**1.67**	**0.09**	**0.00**	**1.89**	**0.06**	**0.00**	**1.91**	**0.01**	**0.01**	**1.92**	**0.00**	**0.02**	**1.98**	**0.01**
240	**0.02**	**1.62**	**0.03**	**0.02**	**1.88**	**0.02**	**0.00**	**1.88**	**0.09**	**0.00**	**1.91**	**0.01**	**0.00**	**1.90**	**0.00**	**0.08**	**1.98**	**0.01**
270	**0.09**	**1.37**	**0.04**	**0.05**	**1.05**	**0.03**	**0.02**	**1.84**	**0.01**	**0.00**	**1.90**	**0.01**	**0.01**	**1.88**	**0.00**	**0.02**	**1.98**	**0.03**

TABLE 6 Results of CG Fault for FI Variation with different locations and FIAs

Angle	0			30			60			90			120			150		
Distance	a	b	c	a	b	c	a	b	c	a	b	c	a	b	c	a	b	c
30	0.06	0.00	**1.42**	0.03	0.01	**1.56**	0.03	0.04	**1.26**	0.03	0.06	**1.82**	0.02	0.31	**0.90**	0.01	0.03	**0.57**
60	0.02	0.00	**1.41**	0.01	0.01	**1.47**	0.02	0.08	**1.28**	0.02	0.04	**1.74**	0.10	0.14	**1.07**	0.01	0.06	**0.81**
90	0.01	0.00	**1.37**	0.01	0.00	**1.39**	0.02	0.08	**1.34**	0.00	0.04	**1.73**	0.05	0.08	**0.94**	0.01	0.03	**0.93**
120	0.02	0.00	**1.31**	0.00	0.00	**1.36**	0.01	0.05	**1.33**	0.01	0.01	**1.75**	0.02	0.03	**0.81**	0.06	0.03	**0.88**
150	0.01	0.00	**1.32**	0.00	0.00	**1.28**	0.00	0.04	**1.16**	0.01	0.04	**1.68**	0.03	0.15	**0.87**	0.05	0.03	**1.03**
180	0.00	0.01	**1.21**	0.00	0.00	**1.26**	0.00	0.01	**1.24**	0.01	0.01	**1.66**	0.06	0.03	**0.99**	0.10	0.08	**0.86**
210	0.07	0.04	**1.22**	0.01	0.00	**1.25**	0.00	0.02	**1.28**	0.02	0.06	**1.67**	0.09	0.07	**1.01**	0.03	0.02	**0.75**
240	0.06	0.05	**1.11**	0.00	0.00	**1.30**	0.00	0.03	**1.24**	0.01	0.03	**1.63**	0.01	0.02	**0.86**	0.01	0.03	**0.64**
270	0.04	0.04	**1.15**	0.00	0.00	**1.30**	0.01	0.01	**1.23**	0.02	0.03	**1.64**	0.02	0.03	**0.92**	0.02	0.02	**0.75**

TABLE 7 Results of AB Fault for FI Variation with different locations and FIAs

Angle	0			30			60			90			120			150		
Distance	a	b	c	a	b	c	a	b	c	a	b	c	a	b	c	a	b	c
30	**1.87**	**1.49**	**0.00**	**1.86**	**1.50**	**0.00**	**1.89**	**1.46**	**0.00**	**1.89**	**1.46**	**0.00**	**1.89**	**1.44**	**0.00**	**1.94**	**1.55**	**0.00**
60	**1.92**	**1.56**	**0.00**	**1.86**	**1.51**	**0.00**	**0.92**	**1.54**	**0.00**	**1.91**	**1.87**	**0.00**	**1.67**	**1.36**	**0.00**	**1.98**	**1.56**	**0.00**
90	**1.83**	**1.50**	**0.00**	**1.84**	**1.51**	**0.00**	**1.90**	**1.48**	**0.00**	**1.81**	**1.88**	**0.00**	**1.66**	**1.56**	**0.00**	**0.99**	**1.45**	**0.00**
120	**1.91**	**1.52**	**0.00**	**1.87**	**1.53**	**0.00**	**1.81**	**1.49**	**0.00**	**1.78**	**1.85**	**0.00**	**1.83**	**1.41**	**0.00**	**1.99**	**1.48**	**0.00**
150	**1.82**	**1.59**	**0.00**	**1.83**	**1.55**	**0.00**	**1.85**	**1.51**	**0.00**	**1.87**	**1.84**	**0.00**	**1.88**	**1.55**	**0.00**	**1.99**	**1.60**	**0.00**
180	**1.82**	**1.57**	**0.00**	**1.85**	**1.57**	**0.00**	**1.83**	**1.53**	**0.00**	**1.82**	**1.73**	**0.00**	**1.84**	**1.48**	**0.00**	**1.99**	**1.54**	**0.00**
210	**1.83**	**1.57**	**0.00**	**1.80**	**1.56**	**0.00**	**1.83**	**1.57**	**0.00**	**1.82**	**1.68**	**0.00**	**1.80**	**1.60**	**0.00**	**1.99**	**1.48**	**0.00**
240	**1.85**	**1.77**	**0.00**	**1.87**	**1.55**	**0.00**	**1.76**	**1.62**	**0.00**	**1.83**	**1.62**	**0.00**	**1.75**	**1.32**	**0.00**	**1.98**	**1.60**	**0.00**
270	**1.82**	**1.57**	**0.00**	**1.81**	**1.65**	**0.00**	**1.82**	**1.55**	**0.00**	**1.82**	**1.62**	**0.00**	**1.83**	**1.53**	**0.00**	**1.96**	**1.55**	**0.00**

TABLE 8 Results of BC Fault for FI Variation with different locations and FIAs

Angle	0			30			60			90			120			150		
Distance	a	b	c	a	b	c	a	b	c	a	b	c	a	b	c	a	b	c
30	**0.00**	**1.90**	**1.10**	**0.00**	**1.94**	**1.98**	**1.96**	**1.95**	**0.00**	**0.00**	**1.96**	**1.96**	**0.00**	**1.95**	**1.95**	**0.00**	**1.93**	**1.91**
60	**0.00**	**1.73**	**1.29**	**0.00**	**1.88**	**1.97**	**1.86**	**1.94**	**0.00**	**0.00**	**1.91**	**1.97**	**0.00**	**1.89**	**1.94**	**0.00**	**1.97**	**1.92**
90	**0.00**	**1.87**	**1.49**	**0.00**	**1.83**	**1.93**	**0.00**	**1.89**	**1.96**	**0.00**	**1.87**	**1.98**	**0.00**	**1.88**	**1.94**	**0.00**	**1.81**	**1.93**
120	**0.00**	**1.83**	**1.49**	**0.00**	**1.80**	**2.00**	**0.00**	**1.82**	**1.99**	**0.00**	**1.84**	**1.98**	**0.00**	**1.83**	**1.97**	**0.00**	**1.81**	**1.93**
150	**0.00**	**1.89**	**1.53**	**0.00**	**1.80**	**1.96**	**0.00**	**1.81**	**1.97**	**0.00**	**1.82**	**1.98**	**0.00**	**1.82**	**1.98**	**0.00**	**1.83**	**1.94**
180	**0.00**	**1.68**	**1.68**	**0.00**	**1.70**	**1.95**	**0.00**	**1.78**	**1.97**	**0.00**	**1.81**	**1.99**	**0.00**	**1.79**	**1.99**	**0.00**	**1.72**	**1.96**
210	**0.00**	**1.79**	**1.71**	**0.00**	**1.80**	**1.96**	**0.00**	**1.87**	**1.99**	**0.00**	**1.81**	**1.99**	**0.00**	**1.81**	**1.99**	**0.00**	**1.86**	**1.99**
240	**0.00**	**1.73**	**1.82**	**0.00**	**1.68**	**1.86**	**0.00**	**1.63**	**1.95**	**0.00**	**1.77**	**1.98**	**0.00**	**1.77**	**2.00**	**0.00**	**1.72**	**2.00**
270	**0.00**	**1.68**	**1.54**	**0.00**	**1.68**	**1.99**	**0.00**	**1.69**	**1.99**	**0.00**	**1.76**	**2.00**	**0.00**	**1.70**	**1.99**	**0.00**	**1.73**	**2.00**

TABLE 9 Results of AC Fault for FI Variation with different locations and FIAs

Angle	0			30			60			90			120			150		
Distance	a	b	c	a	b	c	a	b	c	a	b	c	a	b	c	a	b	c
30	**1.46**	0.04	**1.75**	**1.61**	0.06	**1.92**	**1.98**	0.04	**1.72**	**2.00**	0.01	**1.88**	**1.46**	0.01	**1.65**	**1.46**	0.01	**1.73**
60	**1.47**	0.01	**1.71**	**1.56**	0.08	**1.85**	**1.93**	0.05	**1.77**	**1.93**	0.01	**1.92**	**1.45**	0.01	**1.69**	**1.45**	0.01	**1.70**
90	**1.46**	0.04	**1.70**	**1.45**	0.02	**1.76**	**1.47**	0.07	**1.78**	**1.65**	0.01	**1.95**	**1.46**	0.01	**1.66**	**1.45**	0.01	**1.71**
120	**1.46**	0.01	**1.70**	**1.44**	0.05	**1.77**	**1.44**	0.10	**1.53**	**1.43**	0.02	**1.96**	**1.43**	0.01	**1.78**	**1.45**	0.01	**1.67**
150	**1.61**	0.09	**1.71**	**1.41**	0.07	**1.70**	**1.54**	0.12	**1.73**	**1.44**	0.02	**1.94**	**1.52**	0.01	**1.59**	**1.76**	0.01	**1.62**
180	**1.79**	0.04	**1.60**	**1.89**	0.05	**1.61**	**1.99**	0.04	**1.59**	**1.92**	0.01	**1.98**	**1.60**	0.00	**1.61**	**1.90**	0.01	**1.59**
210	**1.95**	0.06	**1.59**	**1.99**	0.09	**1.60**	**1.97**	0.03	**1.60**	**1.91**	0.01	**1.94**	**1.46**	0.00	**1.58**	**1.27**	0.01	**1.58**
240	**1.98**	0.08	**1.59**	**1.98**	0.07	**1.58**	**1.94**	0.02	**1.57**	**1.41**	0.01	**1.88**	**1.95**	0.01	**1.57**	**1.35**	0.01	**1.57**
270	**1.84**	0.05	**1.57**	**1.93**	0.05	**1.57**	**1.98**	0.02	**1.57**	**1.76**	0.01	**1.77**	**2.00**	0.01	**1.56**	**1.92**	0.02	**1.58**

How to cite this article: Williams K., B. Hoskins, R. Lee, G. Masato, and T. Woollings (2016), A regime analysis of Atlantic winter jet variability applied to evaluate HadGEM3-GC2, *Q.J.R. Meteorol. Soc.*, *2017;00:1–6*.

TABLE 10 Results of ABG Fault for FI Variation with different locations and FIAs

Angle	0			30			60			90			120			150		
Distance	a	b	c	a	b	c	a	b	c	a	b	c	a	b	c	a	b	c
30	**1.64**	**1.11**	**0.00**	**1.62**	**1.98**	**0.15**	**1.65**	**1.93**	**0.34**	**1.65**	**1.98**	**0.42**	**1.67**	**1.91**	**0.01**	**1.65**	**1.94**	**0.05**
60	**1.51**	**1.30**	**0.00**	**1.61**	**1.97**	**0.11**	**1.62**	**1.93**	**0.07**	**1.65**	**1.96**	**0.12**	**1.68**	**1.90**	**0.10**	**1.79**	**1.95**	**0.08**
90	**1.71**	**1.50**	**0.00**	**1.61**	**1.90**	**0.05**	**1.68**	**1.94**	**0.07**	**1.65**	**1.97**	**0.09**	**1.68**	**1.91**	**0.02**	**1.62**	**1.95**	**0.01**
120	**1.68**	**1.50**	**0.00**	**1.60**	**1.99**	**0.01**	**1.64**	**1.99**	**0.04**	**1.66**	**1.97**	**0.05**	**1.66**	**1.94**	**0.03**	**1.65**	**1.94**	**0.02**
150	**1.79**	**1.53**	**0.00**	**1.62**	**1.93**	**0.01**	**1.65**	**1.94**	**0.04**	**1.66**	**1.94**	**0.02**	**1.67**	**1.94**	**0.05**	**1.69**	**1.95**	**0.02**
180	**1.54**	**1.67**	**0.00**	**1.54**	**1.94**	**0.00**	**1.60**	**1.95**	**0.02**	**1.67**	**1.96**	**0.04**	**1.69**	**1.96**	**0.03**	**0.56**	**1.98**	**0.02**
210	**1.67**	**1.72**	**0.00**	**1.67**	**1.92**	**0.00**	**1.74**	**1.96**	**0.02**	**1.67**	**1.96**	**0.04**	**1.58**	**1.94**	**0.10**	**1.74**	**2.00**	**0.02**
240	**1.64**	**1.85**	**0.00**	**1.56**	**1.96**	**0.02**	**1.49**	**1.91**	**0.02**	**1.63**	**1.94**	**0.08**	**1.69**	**1.96**	**0.14**	**1.55**	**1.99**	**0.28**
270	**1.54**	**1.72**	**0.01**	**1.58**	**1.94**	**0.07**	**1.57**	**1.94**	**0.06**	**1.61**	**1.95**	**0.15**	**1.57**	**1.92**	**0.38**	**1.61**	**1.97**	**0.36**

TABLE 11 Results of BCG Fault for FI Variation with different locations and FIAs

Angle	0			30			60			90			120			150		
Distance	a	b	c	a	b	c	a	b	c	a	b	c	a	b	c	a	b	c
30	**0.02**	**0.99**	**0.77**	**0.06**	**1.00**	**1.45**	**0.03**	**1.93**	**1.28**	**0.00**	**1.89**	**1.91**	**0.06**	**1.91**	**1.06**	**0.04**	**1.98**	**0.97**
60	**0.08**	**1.21**	**1.44**	**0.04**	**1.03**	**1.41**	**0.02**	**1.93**	**1.37**	**0.00**	**1.92**	**1.86**	**0.02**	**1.75**	**1.03**	**0.04**	**1.99**	**0.92**
90	**0.03**	**1.42**	**1.30**	**0.01**	**1.02**	**1.38**	**0.01**	**1.91**	**1.33**	**0.00**	**1.85**	**1.87**	**0.01**	**1.73**	**1.06**	**0.03**	**1.99**	**1.09**
120	**0.07**	**1.50**	**1.41**	**0.01**	**0.87**	**1.42**	**0.00**	**1.83**	**1.35**	**0.01**	**1.82**	**1.84**	**0.01**	**1.87**	**1.18**	**0.01**	**1.98**	**1.10**
150	**0.03**	**1.53**	**1.28**	**0.05**	**0.82**	**1.35**	**0.00**	**1.89**	**1.29**	**0.00**	**1.92**	**1.83**	**0.01**	**1.95**	**1.34**	**0.00**	**1.97**	**1.09**
180	**0.01**	**1.62**	**1.42**	**0.08**	**0.70**	**1.42**	**0.01**	**1.86**	**1.38**	**0.00**	**1.86**	**1.72**	**0.06**	**0.03**	**0.99**	**0.00**	**1.98**	**1.08**
210	**0.02**	**1.71**	**1.24**	**0.01**	**0.62**	**1.33**	**0.01**	**1.87**	**1.38**	**0.01**	**1.87**	**1.72**	**0.03**	**1.85**	**0.87**	**0.01**	**1.97**	**1.07**
240	**0.01**	**1.83**	**1.58**	**0.02**	**0.61**	**1.32**	**0.01**	**1.85**	**1.27**	**0.02**	**1.88**	**1.69**	**0.08**	**1.81**	**0.96**	**0.03**	**1.95**	**0.98**
270	**0.05**	**1.87**	**1.30**	**0.05**	**0.61**	**1.43**	**0.03**	**1.87**	**1.27**	**0.04**	**1.87**	**1.70**	**0.01**	**1.88**	**1.01**	**0.03**	**1.97**	**0.95**

TABLE 12 Results of ACG Fault for FI Variation with different locations and FIAs

Angle	0			30			60			90			120			150		
Distance	a	b	c	a	b	c	a	b	c	a	b	c	a	b	c	a	b	c
30	**1.42**	0.03	**1.12**	**1.54**	0.00	**1.39**	**1.36**	0.09	**1.17**	**1.17**	0.04	**1.85**	**0.60**	0.04	**1.09**	**1.44**	0.07	**0.66**
60	**1.32**	0.05	**1.06**	**1.79**	0.01	**1.25**	**1.10**	0.03	**1.29**	**1.46**	0.01	**1.81**	**0.54**	0.02	**1.02**	**1.42**	0.08	**0.79**
90	**1.43**	0.07	**1.21**	**1.56**	0.01	**1.27**	**1.55**	0.01	**1.16**	**0.27**	0.03	**1.84**	**0.63**	0.07	**0.84**	**1.43**	0.06	**0.79**
120	**1.44**	0.02	**1.13**	**1.83**	0.00	**1.07**	**1.44**	0.00	**1.11**	**0.52**	0.01	**1.81**	**0.56**	0.04	**0.97**	**1.43**	0.04	**0.96**
150	**1.43**	0.01	**1.12**	**1.83**	0.01	**1.27**	**1.89**	0.00	**1.09**	**0.57**	0.00	**1.83**	**0.73**	0.02	**1.14**	**1.46**	0.03	**1.02**
180	**1.50**	0.02	**1.12**	**1.86**	0.00	**1.09**	**2.00**	0.01	**1.08**	**0.68**	0.01	**1.69**	**0.41**	0.02	**1.09**	**1.56**	0.04	**0.99**
210	**1.55**	0.01	**1.11**	**1.48**	0.01	**1.18**	**2.00**	0.02	**1.05**	**0.71**	0.02	**1.66**	**0.53**	0.02	**1.01**	**1.37**	0.01	**0.98**
240	**1.55**	0.08	**1.16**	**1.48**	0.02	**1.13**	**1.94**	0.10	**1.28**	**0.52**	0.01	**1.56**	**0.53**	0.05	**1.01**	**1.40**	0.01	**1.01**
270	**1.68**	0.04	**1.15**	**1.56**	0.02	**1.08**	**1.91**	0.04	**1.17**	**0.54**	0.09	**1.65**	**0.96**	0.08	**0.98**	**1.70**	0.01	**0.92**

TABLE 13 Results of ABCG Fault for FI Variation with different locations and FIAs

Angle	0			30			60			90			120			150		
Distance	a	b	c	a	b	c	a	b	c	a	b	c	a	b	c	a	b	c
30	**1.50**	**1.10**	**0.71**	**1.93**	**1.92**	**1.30**	**1.98**	**1.91**	**1.24**	**1.50**	**1.91**	**1.91**	**1.51**	**1.91**	**1.24**	**1.50**	**1.95**	**1.27**
60	**1.35**	**1.30**	**0.63**	**1.67**	**1.94**	**1.29**	**1.99**	**1.91**	**1.33**	**1.56**	**1.92**	**1.85**	**1.50**	**1.82**	**1.15**	**1.57**	**1.96**	**1.28**
90	**1.54**	**1.51**	**0.58**	**1.98**	**1.86**	**1.29**	**1.99**	**1.91**	**1.23**	**1.47**	**1.90**	**1.86**	**1.50**	**1.80**	**1.31**	**1.47**	**1.95**	**1.21**
120	**1.51**	**1.50**	**0.56**	**1.76**	**1.95**	**1.22**	**2.00**	**1.92**	**1.15**	**1.49**	**1.89**	**1.83**	**1.50**	**1.90**	**1.23**	**1.49**	**1.94**	**1.24**
150	**1.59**	**1.53**	**0.67**	**1.65**	**1.88**	**1.24**	**1.98**	**1.90**	**1.27**	**1.48**	**1.91**	**1.83**	**1.50**	**1.92**	**1.39**	**1.50**	**1.95**	**1.31**
180	**1.46**	**1.67**	**0.61**	**1.64**	**1.90**	**1.24**	**1.86**	**1.91**	**1.18**	**1.53**	**1.91**	**1.71**	**1.54**	**1.91**	**1.30**	**1.49**	**1.96**	**1.27**
210	**1.53**	**1.67**	**0.62**	**1.88**	**1.88**	**1.96**	**1.91**	**1.21**	**1.61**	**1.91**	**1.69**	**1.34**	**1.91**	**1.31**	**1.48**	**1.99**	**1.22**	**1.27**
240	**1.49**	**1.80**	**0.59**	**1.46**	**1.93**	**1.23**	**1.77**	**1.88**	**1.29**	**1.57**	**1.90**	**1.61**	**1.57**	**1.89**	**1.09**	**1.35**	**1.93**	**1.36**
270	**1.49**	**1.90**	**0.66**	**1.48**	**1.90**	**1.26**	**1.96**	**1.91**	**1.24**	**1.56**	**1.91**	**1.68**	**1.50**	**1.91**	**1.26**	**1.51**	**1.97**	**1.26**